Cyclophilin D inactivation protects axons in experimental autoimmune encephalomyelitis, an animal model of multiple sclerosis

Michael Forte*†, Bruce G. Gold‡, Gail Marracci‡§, Priya Chaudhary‡, Emy Basso¶, Dustin Johnsen*, Xiaolin Yu‡, Jonathan Fowlkes*, Micha Rahder‡, Katie Stem‡, Paolo Bernardi¶, and Dennis Bourdette‡†

*Vollum Institute and ‡Department of Neurology, Oregon Health and Science University, Portland, OR 97239; ¶Department of Biomedical Sciences, University of Padova, I-35121 Padova, Italy; and §Department of Veterans Affairs, Portland, OR 97239

Communicated by Douglas C. Wallace, University of California, Irvine College of Medicine, Irvine, CA, March 12, 2007 (received for review October 19, 2006)

Multiple sclerosis (MS) is the leading cause of neurological disability in young adults, affecting some two million people worldwide. Traditionally, MS has been considered a chronic, inflammatory disorder of the central white matter in which ensuing demyelination results in physical disability [Frohman EM, Racke MK, Raine CS (2006) *N Engl J Med* 354:942–955]. More recently, MS has become increasingly viewed as a neurodegenerative disorder in which neuronal loss, axonal injury, and atrophy of the CNS lead to permanent neurological and clinical disability. Although axonal pathology and loss in MS has been recognized for >100 years, very little is known about the underlying molecular mechanisms. Progressive axonal loss in MS may stem from a cascade of ionic imbalances initiated by inflammation, leading to mitochondrial dysfunction and energetic deficits that result in mitochondrial and cellular Ca^{2+} overload. In a murine disease model, experimental autoimmune encephalomyelitis (EAE) mice lacking cyclophilin D (CyPD), a key regulator of the mitochondrial permeability transition pore (PTP), developed EAE, but unlike WT mice, they partially recovered. Examination of the spinal cords of CyPD-knockout mice revealed a striking preservation of axons, despite a similar extent of inflammation. Furthermore, neurons prepared from CyPD-knockout animals were resistant to reactive oxygen and nitrogen species thought to mediate axonal damage in EAE and MS, and brain mitochondria lacking CyPD sequestered substantially higher levels of Ca^{2+}. Our results directly implicate pathological activation of the mitochondrial PTP in the axonal damage occurring during MS and identify CyPD, as well as the PTP, as a potential target for MS neuroprotective therapies.

axonal degeneration | mitochondria | permeability transition | calcium

Multiple sclerosis (MS) is the leading cause of neurological disability in young adults, affecting some 2 million people worldwide. Traditionally, MS has been considered a chronic, inflammatory disorder of the CNS in which ensuing demyelination results in physical disability (1). However, demyelination itself produces clinical deficits that can remit because of remyelination and reorganization of the ion channel repertoire in axons that restores action potential conduction along chronically demyelinated axons (2, 3). More recently, MS has become increasingly viewed as a neurodegenerative disorder in which neuronal loss, axonal injury, and atrophy of the CNS occur progressively from the start of the disease (4, 5). Permanent neurological and clinical disability, especially in patients with long disease duration, is thought to develop when a threshold of axonal loss is reached and CNS compensatory responses are exhausted (4, 6). Data from both humans and experimental animal models of MS support the idea of a causal relationship among inflammation, axonal loss, and permanent neurological disability (6–8).

Although axonal degeneration is now recognized as critical to permanent disability in MS, relatively little is known about the underlying molecular mechanisms that are responsible for this pathological process. Most current hypotheses invoke a complex cascade of interrelated processes leading to mitochondrial dysfunction (4, 9, 10). For example, compounds generated in response to inflammation (e.g., reactive oxygen and nitrogen species) inhibit mitochondrial electron transport, resulting in axonal energy deficits (11, 12). Recent reports have documented impaired activity of several mitochondrial respiratory complexes in MS plaques (10). This complex interplay between a variety of molecular pathways has been proposed to ultimately result in neuronal Ca^{2+} overload and the activation of Ca^{2+}-activated proteolytic processes that produce axonal injury (13).

It is now well established that mitochondria play a pivotal role in cell survival in large part because of their participation in the dynamic regulation of cellular Ca^{2+}; mitochondria accumulate cytoplasmic Ca^{2+} whenever the local cytoplasmic-free Ca^{2+} rises above a critical set point and then slowly release Ca^{2+} when normal cytoplasmic Ca^{2+} levels are restored (14–16). Under normal conditions, the accumulation of Ca^{2+} into mitochondria stimulates oxidative metabolism (14, 15). Consequently, mitochondria contain a variety of molecular complexes that mediate, and precisely regulate, the uptake and release of Ca^{2+}. Whereas a number of cotransporters mediate Ca^{2+} efflux from mitochondria, Ca^{2+} efflux is also driven by the activation of an incompletely characterized complex of proteins called the permeability transition pore (PTP) (17). In intact cells, transient activation of the PTP is likely to mediate the fast release of Ca^{2+} from the mitochondrion under normal conditions (18–21). However, overload of mitochondria with Ca^{2+} as a consequence of pathological stimuli results in inappropriate activation of the PTP, resulting in dramatic alterations in mitochondrial function, including decreased ATP production and increased generation of reactive oxygen (22–24). Thus, the excess axonal Ca^{2+} postulated to trigger the axonal injury observed in MS would be predicted to lead to elevated levels of Ca^{2+} within axonal mitochondria, unregulated activation of the PTP, and consequent mitochondrial dysfunction.

Although the question of which molecular components form the PTP has remained controversial, extensive biochemical, functional, and genetic data implicate a nuclearly encoded

Author contributions: M.F., P.B., and D.B. designed research; J.F., M.R., and K.S. performed research; B.G.G., G.M., P.C., E.B., D.J., X.Y., and J.F. contributed new reagents/analytic tools; M.F., B.G.G., G.M., P.C., P.B., and D.B. analyzed data; and M.F. and D.B. wrote the paper.

The authors declare no conflict of interest.

Freely available online through the PNAS open access option.

Abbreviations: CsA, cyclosporin A; CyPD, cyclophilin D; CyPD-KO, CyPD-knockout; DETA-NO, (*Z*)-1-[2-aminoethyl]-*N*-(2-ammonioethyl)amino]diazen-1-ium 1,2-diolate; EAE, experimental autoimmune encephalomyelitis; MOG, myelin oligodendrocyte glycoprotein; MS, multiple sclerosis; NF, neurofilament; NF-P, phosphorylated neurofilament; PTP, permeability transition pore.

†To whom correspondence should be addressed. E-mail: forte@ohsu.edu or bourdett@ohsu.edu.

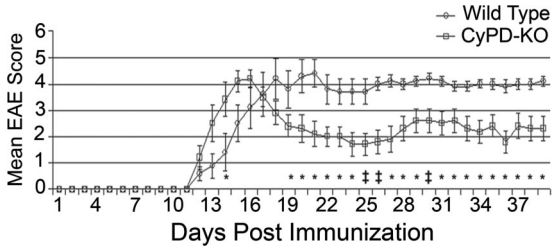

Fig. 1. CyPD-KO mice have a less severe EAE disease course than WT (C57BL/6) mice. Mice were immunized with MOG 35-55 peptide as outlined in *Materials and Methods*. Mice were monitored and scored daily by using a nine-point system. The experiment was terminated after 39 days. Open circles represent the mean daily EAE score for WT mice. Closed squares represent the mean daily EAE score for CyPD-KO mice. Error bars indicate the SEM. Daily EAE scores were compared between the WT and CyPD-KO groups and analyzed by the Mann–Whitney *U* test. *, $P < 0.05$; ‡, $P < 0.005$. $n = 10$ in each group.

mitochondrial cyclophilin, cyclophilin D (CyPD), as a key regulator of the function of the PTP (25). Thus, genetic inactivation of the murine *Ppif* gene encoding CyPD [CyPD-knockout (CyPD-KO)], has demonstrated that the absence of CyPD dramatically increased the threshold Ca^{2+} load required to open the PTP in mitochondria prepared from CyPD-KO liver (26–29). Furthermore, despite the absence of CyPD, mitochondria from CyPD-KO mice displayed basal-, ADP-, and uncoupler-stimulated rates of respiration that were indistinguishable from mitochondria prepared from WT mice, demonstrating that the absence of CyPD does not affect energy conservation and ATP synthesis (27). In addition, murine embryonic fibroblasts prepared from CyPD-KO mice show an increased resistance to both oxidative stress and elevated cytoplasmic Ca^{2+} levels compared with WT cells (27–29). By extension, whole-animal studies demonstrated the striking resistance of CyPD-KO mice to ischemic brain injury, which results in the generation of reactive oxygen species and Ca^{2+} overload (27). Consequently, given the characteristics of cells and animals lacking CyPD, and their resistance to pathological states resulting in Ca^{2+} overload, we assessed the response of mice missing CyPD ($Ppif^{-/-}$) following induction of experimental autoimmune encephalomyelitis (EAE), a murine model of MS (30, 31).

Results

Mice Missing CyPD Recover Following Induction of EAE. Given the differences observed in various inbred mouse lines on the progression and magnitude of disease following induction of EAE (31), we initially backcrossed CyPD-KO animals to C57BL/6 mice eight times to place the CyPD-KO mutation in an isogenic C57BL/6 background. To induce EAE, we immunized isogenic WT C57BL/6 control and CyPD-KO mice with myelin oligodendrocyte glycoprotein (MOG) 35-55 peptide following standard protocols and initially assessed disease course in both groups by daily observation of clinical progression (Fig. 1) (30). Beginning 12 days after immunization, both WT and CyPD-KO mice developed clinical EAE (manifested as limb weakness and paralysis) of similar severity, although the CyPD-KO mice tended to develop maximum paralysis earlier than the WT mice. After developing EAE, the WT mice did not recover, as is typical for MOG 35-55 peptide-induced EAE in C57BL/6 mice (31). However, beginning on day 17 after immunization, the CyPD-KO mice began to improve clinically. By the end of the experiment, 39 days after immunization, the CyPD-KO mice were significantly better, clinically, than the WT mice (mean total EAE score of 68 versus 100, $P = 0.04$); similar clinical outcomes were obtained in two subsequent experiments. Thus, CyPD-KO mice initially develop EAE as do WT controls but, unlike WT mice, partially recover.

Axons in CyPD-KO Mice Are Preserved Following EAE. Tissue damage in EAE in WT C57BL/6 mice manifests as multifocal areas in the white matter of the caudal spinal cord, with prominent axonal damage consisting of degenerating axons and reduction in axonal density. To assess axonal integrity following induction of EAE, 39 days after immunization, randomly selected WT and CyPD-KO mice were perfused with glutaraldehyde and their thoracic spinal cords processed for quantitative morphology. In plastic-embedded toluidine blue-stained sections, we quantified the percentage area of white matter in the thoracic spinal cord containing axonal damage. In WT mice with EAE, a mean of 36.7% of the lateral/ventral white matter and 17.6% of the dorsal white matter exhibited a mixture of pathological changes when compared with naïve controls, including axons undergoing Wallerian-like degeneration, reduced nerve fiber density, and occasional demyelinated axons (Fig. 2 *A* and *B*). However, CyPD-KO mice with EAE showed significantly less axonal damage than WT controls; a mean of 7.5% of lateral/ventral (80% reduction) and 7.1% of dorsal (60% reduction) white matter in CyPD-KO mice showed axonal injury ($P = 0.002$ and $P = 0.001$, respectively) (Fig. 2 *C* and *D*). Higher-power views of areas of tissue damage demonstrated extensive axonal degeneration and reduction in axonal density in WT mice with EAE (Fig. 2 *E–G*). At this level, degenerating axons are present within lesions in CyPD-KO mice, but to a much lower extent than observed in WT animals, with the nerve fiber densities more like that of normal spinal cord white matter (compare Fig. 2 *E* and *G*). These results demonstrate that, compared with WT mice, axons in CyPD-KO mice are protected from the damage resulting from the induction of EAE. Moreover, even in areas of injury, CyPD-KO mice with EAE had fewer degenerating axons and a more normal nerve fiber density.

To further evaluate axonal protection in CyPD-KO mice following the induction of EAE, we used immunohistochemical methods to assess the levels of neurofilament phosphorylation (NF-P). In normal axons, neurofilaments (NFs) are highly phosphorylated; consequently, dephosphorylation of NFs has been used to monitor axonal damage in MS and EAE (5, 32). Again, 39 days following induction of EAE, fixed sections were prepared from the thoracic spinal cords of a different set of randomly selected WT and CyPD-KO animals and immunostained with a mixture of antibodies specifically directed to NF-P. Sections from WT mice with EAE showed a marked reduction in staining for NF-P (Fig. 3 *A–C*). Comparable sections from CyPD-KO mice with EAE exhibited little reduction in the level of NF-P, reflecting significant preservation of axonal integrity (Fig. 3*D*). Quantification of these differences demonstrated that the percentage area of the lateral/ventral and dorsal thoracic spinal cord showing axonal damage, as assessed by NF-P staining, was significantly reduced in CyPD-KO mice; the area of damage in spinal cords from WT and CyPD-KO was 25% and 2.2% for the lateral/ventral regions and 15% and 3.65% for the dorsal regions, respectively (Fig. 3*E*; $P = 0.001$ and $P = 0.025$). These results support the conclusions generated from quantitative morphological analysis and demonstrate significant axonal preservation in CyPD-KO mice following induction of EAE.

EAE Generates Similar Levels of Inflammation in CyPD-KO Mice. The development of EAE following immunization of C57BL/6 mice with MOG 35-55 peptide requires the evolution of inflammatory infiltrates composed principally of $CD4^+$ and $CD8^+$ T cells and $CD11b^+$ macrophages/microglial cells within the spinal cord. Consequently, it may be that the reduction in axonal damage and improvement in clinical EAE observed in CyPD-KO mice could reflect a difference in the immune response or extent of inflammation within the spinal cord of CyPD-KO animals. To investigate this possibility, we assessed the peripheral immune response to MOG 35-55 peptide and the inflammation in

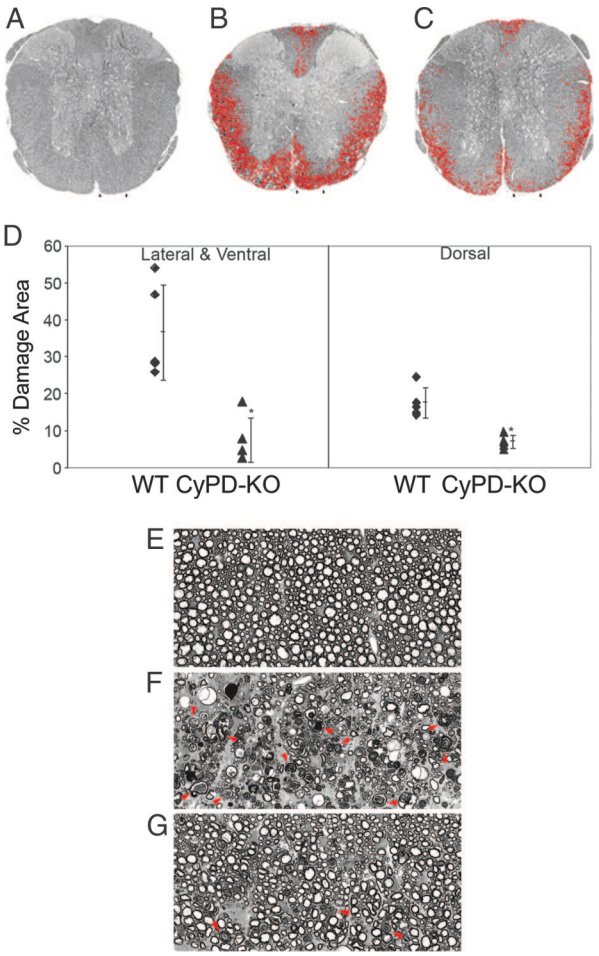

Fig. 2. Spinal cords of CyPD-KO mice show less damage following induction of EAE than WT mice. Low-power (×30) view of thoracic spinal cord sections from naïve (*A*), WT (*B*), and CyPD-KO (*C*) mice 39 days after immunization with MOG 35-55. Spinal cords are stained with toluidine blue, and the areas of tissue damage in white matter are circled in red. (Arrows demarcate the areas magnified and presented in *E–G*). (*D*) Morphometric analyses of the percentage of the area protected in EAE WT and CyPD-KO lateral and ventral and dorsal spinal cord sections. Measurements were made of the damaged and total (damaged and nondamaged) spinal cord columns ($n = 4$ in each group) as detailed in *Materials and Methods*. *, $P < 0.002$. Higher power (×240) views of thoracic spinal cord sections from naïve (*E*), WT (*F*), and CyPD-KO (*G*) mice. (*E*) Normal spinal cord white matter morphology. (*F*) Representative area of tissue damage from WT mouse with EAE. (*G*) Representative area of tissue damage from a CyPD-KO mouse with EAE. Compared with WT, relatively few axons are undergoing Wallerian-like degeneration, and the axonal density is more normal. Arrowheads indicate examples of fibers undergoing Wallerian-like degeneration.

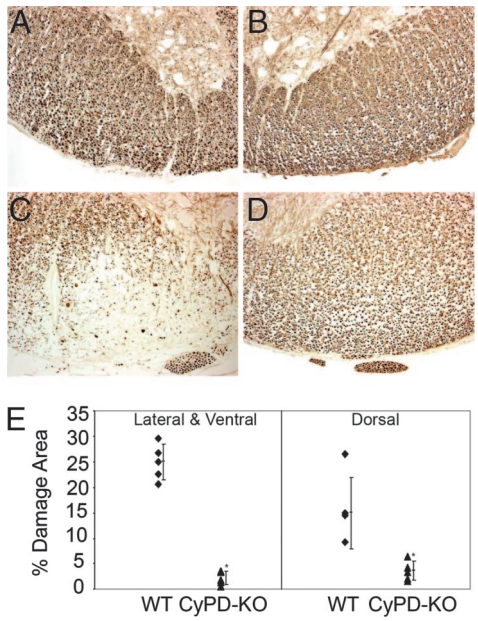

Fig. 3. Phosphorylated neurofilament staining of WT and CyPD-KO spinal cords following induction of EAE. Paraffin-embedded thoracic spinal cord sections were immunostained for phosphorylated NFs from WT naïve (*A*), CyPD-KO naïve (*B*), WT (*C*), and CyPD-KO (*D*) mice 39 days after immunization with MOG 35-55 peptide. Note the marked reduction in immunostaining in the WT mouse spinal cord and relatively normal staining in the CyPD-KO mouse spinal cord. (Scale bar: 50 μm.) (*E*) Dot plot representation of the mean percentage area of damage in the white matter (naïve mice not shown). From these data, cumulative lesion area percentages were calculated for the lateral/ventral and dorsal columns. *, $P < 0.025$.

CyPD-KO and WT mice. Fifteen days after immunization with MOG 35-55 peptide (during acute EAE; Fig. 1), lymph nodes from WT and CyPD-KO mice were removed and lymph node cell cultures established. After 48 h, cells were pulsed with [^{3}H]thymidine and harvested 18 h later to assess proliferation. There were no significant differences in proliferative responses between WT and CyPD-KO lymph node cell cultures following stimulation with MOG 35-55 peptide (Fig. 4*A*). In addition, using immunofluorescence staining, we quantified the levels of CD4, CD8, and CD11b cells in lumbar spinal cord sections from WT and CyPD-KO naïve mice and those with EAE 15 days after immunization with MOG 35-55 peptide (Fig. 4 *B–I*). As expected, there were significantly elevated levels of CD4, CD8, and CD11b immunofluorescence in the both WT and CyPD-KO animals with EAE, reflecting spinal cord infiltration with CD4$^+$ and CD8$^+$ T cells and macrophages/microglial cells. As is typical for EAE, there was considerably more staining with CD11b, reflecting the predominance of macrophages/microglial cells in the inflammatory infiltrates. Importantly, there was no statistically significant difference in CD4, CD8, or CD11b staining in spinal cord sections prepared from WT and CyPD-KO mice with EAE at either day 15 or 39 (Fig. 4 *J–L*). Thus, by two different measures, the inflammatory response of WT and CyPD-KO mice with EAE was comparable, suggesting that axonal protection observed in CyPD-KO mice is not primarily due to blunted inflammatory reactions that might be associated with the elimination of this protein. In this regard, it is worth noting that the CyPD-KO mice tended to develop the same level of peak disease earlier than WT mice (Fig. 1), suggesting a somewhat more robust, rather than impaired, inflammatory response.

CyPD-KO Neurons Are Resistant to Reactive Oxygen and Nitrogen Challenges and Brain Mitochondria from CyPD-KO Mice Accumulate Higher Levels of Ca^{2+}. Reactive oxygen and nitrogen generated during inflammation are believed to be key mediators of the mitochondrial dysfunction and ensuing axonal damage in EAE and MS (11). Accordingly, we examined the relative sensitivity of neurons prepared from CyPD-KO mice to reactive oxygen and nitrogen. As shown in Fig. 5 *A* and *B*, cortical neurons prepared from P0 CyPD-KO animals show a dramatically increased resistance to agents leading to elevated reactive oxygen (H_2O_2) and elevated reactive nitrogen [(*Z*)-1-[*N*-(2-aminoethyl)-*N*-(2-ammonioethyl)amino]diazen-1-ium 1,2-dioate (DETA-NO)] when compared with neurons prepared from WT animals. These results are consistent with the idea that the axonal protection observed in CyPD-KO mice with EAE is due to the inherent resistance of mutant neurons to these inflammatory mediators

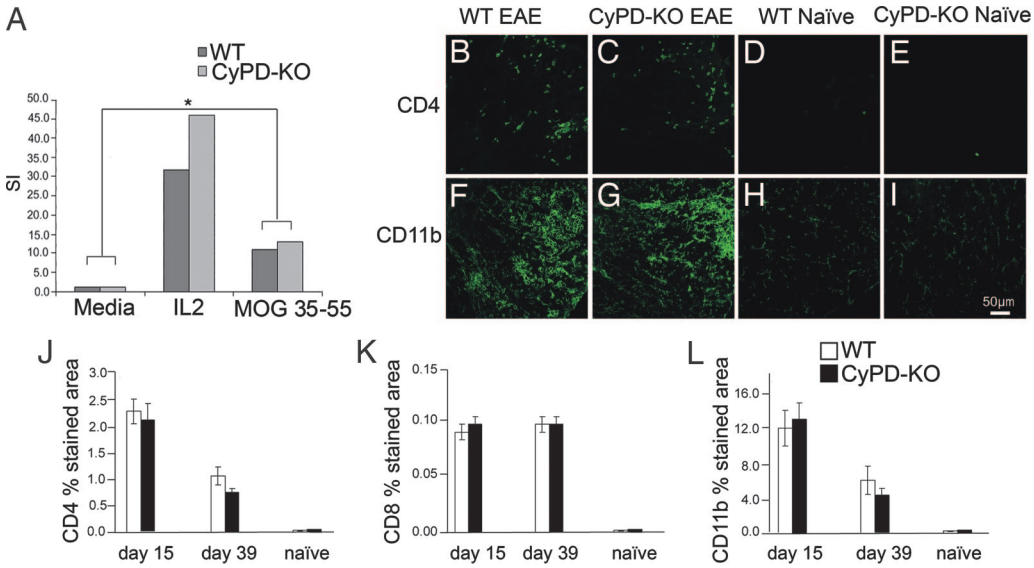

Fig. 4. CyPD-KO and WT mice with EAE have similar degrees of inflammation within the spinal cord. (*A*) Wild-type C57BL/6 and CyPD-KO mice were immunized with MOG 35-55 (200 μg per mouse) in complete Freund's adjuvant (400 μg of *Mycobacterium tuberculosis* per mouse) and were administered pertussis toxin at 25 ng per mouse on day 0 and 66 ng per mouse on day 2 after immunization. Mice were killed during acute disease at day 17, and draining lymph nodes were harvested for proliferation assays. Single cell suspensions of lymphocytes were treated with IL-2 and MOG 35-55 (25 μg/ml) or saline control. Cells were incubated at 37°C and labeled with [^{3}H]thymidine for the last 18 h of a 72-h culture period. *, $P < 0.05$. (*B–I*) Fifty-micrometer sections of the lumbar spinal cord were stained with anti-CD4 (*Upper*) and anti-CD11b (*Lower*) at 15 days after immunization with MOG 35-55 peptide. (*B* and *F*), WT; (*C* and *G*), CyPD-KO; (*D* and *H*), naïve WT; and (*E* and *I*), naïve CyPD-KO. Note that there is no difference in the CD4 and CD11b staining between CyPD-KO and WT spinal cord ($n = 4$ mice in each group). (*J–L*) Quantification of inflammatory cell levels in spinal cord sections. Percentage area stained with anti-CD4 (*J*), anti-CD8 (*K*), and anti-CD11b (*L*). (Scale bar: 50 μm.) Dorsal, lateral, and ventral spinal cord (white matter) were photographed using the ×40 objective on a laser scanning confocal microscope. All image processing and analysis was done as outlined in *Materials and Methods*.

of axonal disruption. To elucidate the mechanisms that might underlie the resistance of CyPD-KO axons and neurons to the induction of EAE, we tested the intrinsic properties of the PTP in brain mitochondria prepared from CyPD-KO mice. Specifically, we determined the threshold Ca^{2+} required to open the PTP in a population of brain mitochondria (Ca^{2+} retention capacity). This test assesses the ability of mitochondria to take up Ca^{2+} by measuring the disappearance of extramitochondrial free Ca^{2+} from the media after the addition of pulses of Ca^{2+} (e.g., ref. 26). As shown in Fig. 5*C*, the Ca^{2+} retention capacity of mitochondria prepared from brains of CyPD-KO mice was significantly increased when compared with mitochondria prepared from WT mouse brains and was similar to that observed in WT mitochondria treated with cyclosporin A (CsA), an inhibitor of the PTP that binds to CyPD (25, 26). In addition, the retention capacity of CyPD-KO mitochondria was not altered by the addition of CsA as expected because CyPD is the molecular target of CsA (26–29) Thus, brain mitochondria lacking CyPD are able to more effectively deal with Ca^{2+} challenges than WT brain mitochondria.

Discussion

Although axonal pathology and loss in MS has been recognized for >100 years (33), very little is known about the underlying molecular mechanisms. Recently, the role of axonal Ca^{2+} overload and the ensuing mitochondrial dysfunction in the axonal destruction accompanying MS has been the subject of much speculation. However, little in the way of direct evidence has implicated either of these processes in events leading to the permanent disability associated with MS. If accurate, this hypothesis would predict that identification of molecular targets that would preserve mitochondrial function in the face of disease challenges would be therapeutically useful in preventing the axonal damage accompanying MS. Because the cause and pathogenesis of MS in humans are only poorly understood, we examined the consequences of a mutation eliminating expression of mitochondrial CyPD in a mouse model of MS, EAE. In this model, immunization with peptides found in myelin proteins leads to disease that shares clinical and neuropathological changes observed in human MS (34, 35). Although artificial immunization may not necessarily reproduce all of the pathogenic mechanisms operating in the human disease, the validity of such models has been repeatedly confirmed; most importantly, the study of EAE has led to the development of three of the currently available MS therapies (35, 36). In addition, because different inbred mouse lines exhibit a variety of pathological responses to immunization with myelin peptides (31), we assessed consequences of the absence of CyPD on the progression of EAE in mice in which the CyPD-KO mutation has been backcrossed into an isogenic C57BL/6 background. The results presented here demonstrate that neurons missing CyPD, a key regulator of the PTP, are resistant to agents thought to be the mediators of axonal degeneration observed in both EAE and MS and have mitochondria that are able to more effectively handle elevated Ca^{2+}. Consistent with this neuronal resistance, animals missing CyPD are able to recover, clinically, following the induction of EAE. A similar resistance to the development of EAE has also been observed in mice missing osteopontin (37, 38) and IL-17 (39). However, in these mutants, attenuated EAE has been attributed to abnormal T cell responses and alterations in cytokine production resulting from the lack of each protein. Furthermore, the impact of the absence of each protein on axonal integrity following induction of EAE was not assessed. Here, axons in CyPD-KO animals have significantly reduced axonal damage, despite levels of inflammation similar to that of WT animals following induction of EAE.

Given the profound effect that Ca^{2+} overload can have on neuronal survival, our results support a model by which disruption of mitochondrial function by inflammatory agents associated with EAE and MS may directly lead to the neuronal cell

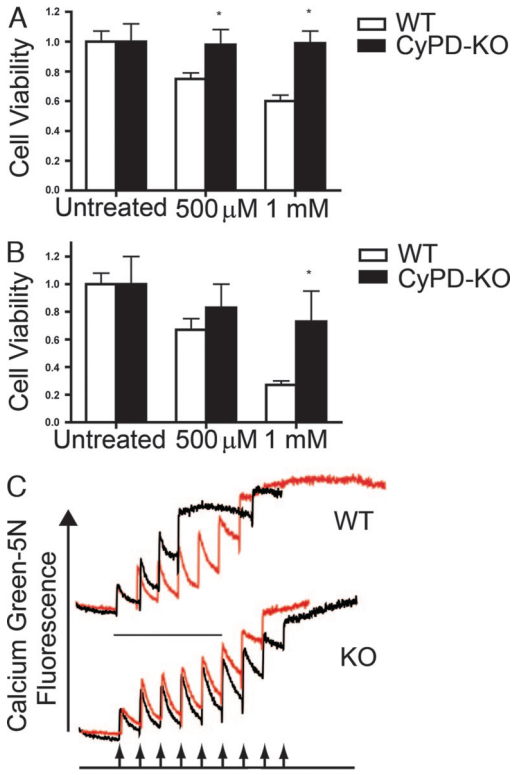

Fig. 5. CyPD-KO neurons are resistant to reactive oxygen and nitrogen, and brain mitochondria lacking CyPD accumulate more Ca^{2+}. Effects of H_2O_2 (*A*) and (*Z*)-1-[*N*-(2-aminoethyl)-*N*-(2-ammonioethyl)amino]diazen-1-ium 1,2-dioate (DETA-NO) (*B*) on the viability of cortical neurons prepared from WT and CyPD-KO mice. P0 cortical neurons were prepared, treated, and viability was determined as outlined in *Materials and Methods by using* the Biotium assay kit for live/dead animal cells (Biotium). Data represent mean ± SD. *, $P < 0.01$. Ca^{2+} uptake by WT and CyPD-KO mitochondria. (*C*) Mitochondria were prepared from WT and CyPD-KO (designated here as ''KO'') brains, and calcium retention capacities were assayed as outlined in *Materials and Methods*. Experiments were started by the addition of 1 mg of mitochondrial protein to 2 ml of standard reaction buffer in the presence of Ca^{2+}. (*Upper*) WT mitochondria. (*Lower*) CyPD-KO mitochondria. In each, black traces represent untreated mitochondria and red traces represent mitochondria assayed in the presence of 1.6 μM CsA. As shown, CyPD mitochondria take up roughly 2-fold more Ca^{2+} than WT mitochondria before the activation of the PTP, and activation of the PTP in CyPD-KO mitochondria is not altered by CsA.

death and the ensuing axonal damage that underlie the generation of permanent disability. In this context, our data show that elimination of CyPD enhances the ability of mitochondria to sequester Ca^{2+} over time, thereby protecting mitochondria against aberrantly high levels of cytoplasmic Ca^{2+} in neurons and axons that occurs in these diseases. Thus, our results provide evidence of direct links between mitochondrial function, Ca^{2+} overload, and axonal destruction during EAE, and by extension, MS. In addition, present therapeutic interventions for MS depend exclusively on modulators of the immune/inflammatory response during disease progression, which may only indirectly be capable of modulating pathways leading to axonal destruction (40, 41). Taken together, our findings suggest that inhibitors of CyPD and the PTP may represent important new therapeutic targets for the prevention of axonal degeneration in MS. CyPD, as one molecular target in the PTP, can be inhibited by CsA. Indeed, CsA has been shown to reduce tissue injury in EAE, although differentiating its neuroprotective effects from its immunosuppressive effects was not possible (42, 43). However, the toxicity associated with long-term CsA use has prevented its use as a treatment for MS (44). CsA derivatives that are not immunosuppressive and are less toxic have been developed (45, 46). Based on our results, compounds that are able to inhibit the PTP by inactivation of CyPD specifically, as well as other drugs that modulate the PTP, would seem to warrant investigation as neuroprotective therapies in MS.

Materials and Methods

Induction and Assessment of Active EAE. CyPD-KO mice were generated and backcrossed eight times into the C57BL/6 background as described in Basso *et al.* (26). Isogenic CyPD-KO and C57BL/6 (The Jackson Laboratory, Bar Harbor, ME) control female mice were immunized with 200 μg of MOG 35-55 peptide in complete Freund's adjuvant containing 400 μg of *Mycobacterium tuberculosis* per mouse by s.c. injection. Pertussis toxin was administered i.p. at day 0 (25 ng per mouse) and day 2 (66 ng per mouse) after immunization. Mice were scored daily for EAE by using a 9-point scale (0, no paralysis; 1, limp tail with minimal hind limb weakness; 2, mild hind limb weakness; 3, moderate hind limb weakness; 4, moderately severe hind limb weakness; 5, severe hind limb weakness; 6, complete hind limb paralysis; 7, hind limb paralysis with mild forelimb weakness; 8, hind limb paralysis with moderate forelimb weakness; and 9, hind paralysis with severe forelimb weakness).

Quantitative Morphological Determination of Percentage of White Matter Tissue Damage. Mice were deeply anesthetized with isoflurane, heparinized, and perfused with 5% glutaraldehyde, and spinal cords were dissected as previously described (47). Tissue samples were postfixed with 1% osmium. Semithin sections (0.5 μm) were stained with toluidine blue and photographed at ×25 magnification. Tissue sections were then analyzed blinded to treatment status. The percentage of the spinal cord showing damage was determined in the midthoracic cord. Photomontages (final magnification, ×100) of the entire spinal cord and areas containing damaged fibers were measured by using a SummaSketch III (Summagraphics, Fairfield, CT) digitizing tablet and BIOQUANT Classic 95 software (R & M Biometrics, Nashville, TN). Measurements were taken of the total area (damaged and nondamaged) and the cumulative percentage area of lesions was calculated for dorsal and ventral/lateral columns.

Immunohistochemical Studies. Mice were perfused with 4% paraformaldehyde and 1- to 2-mm lengths of spinal cord were processed for sectioning as previously described (43, 47). For phosphorylated NF staining, spinal cord sections were blocked and stained with anti-phosphorylated NF, SMI312 (Sternberger Monoclonals, Lutherville, MD). Following incubation in goat anti-mouse secondary antibody and incubation in mouse peroxidase–antiperoxidase, immunoreactivity was visualized with 0.05% diaminobenzidine tetrahydrochloride/0.01% hydrogen peroxide, examined by light microscopy, and photographed and analyzed as described above. Statistical significance was determined by using one-way ANOVA followed by Newman–Keuls multiple comparisons tests (WINKS 4.62 professional edition; Texasoft, Dallas, TX); significance was defined as $P < 0.05$.

For quantitative immunofluorescent analyses, three 50-μm sections from each lumbar spinal cord region were randomly selected for antibody staining. In brief, the sections were permeabilized, washed, blocked (0.5% fish skin gelatin/3% BSA) in PBS, and then incubated with primary antibody at 4°C overnight. After incubation in secondary antibody, sections were mounted in Prolong Gold antifade and analyzed with an Olympus laser scanning confocal microscope by using Fluoview software, version 3 (Olympus, Melville, NY). Primary antibodies anti-CD4 and -CD8 (PharMingen, San Diego, CA; 1:25 dilution) were used to identify T cells; anti-Mac-1 (CD11b; Leinco Technologies, St. Louis, MO; 1:75 dilution) was used as a microglial/macrophage marker. Secondary antibody Alexa Fluor 488 donkey anti-rat IgG (Invitrogen, Carls-

bad, CA; 1:200 dilution) was used. To quantify immunofluorescence, dorsal, lateral, and ventral spinal cord sections were photographed (×40) on a laser scanning confocal microscope. Data analyses were assessed from 24 raw images from four mice in each group (MetaMorph software, v6.2; Molecular Devices, Sunnyvale, CA). The average background fluorescence was determined from several areas containing unlabeled regions of the spinal cord, from naïve spinal cords, and from sections incubated in secondary antibody only. Data analyses were done in a blinded manner. The percentage of threshold area was compared between different groups. Statistical significance was calculated by using the nonparametric Mann–Whitney *U* test.

Preparation, Treatment and Analysis of Neuronal Cultures. Cortical neurons were obtained from dissected brains of newborn (P0) WT and CyPD-KO animals by published protocols (48, 49). Briefly, individual cells were dissociated by using trypsin in Hanks's balanced salt solution lacking Ca^{2+} and Mg^{2+} at 37°C and followed by a wash in Hanks's balanced salt solution containing trypsin inhibitor. Cells were then dissociated mechanically in Neurobasal A medium by repeated passage through a pipette tip and washed twice in serum-free neurobasal medium plus B27 supplement (Invitrogen). Cells were then mixed with an equal volume of trypan blue, and the number of dye-excluding cells counted in a hemocytometer. Viable cells were then plated on poly(D-lysine)-coated dishes or coverslips at 1.1×10^5 cells per cm^2 in serum-free neurobasal medium plus B27 supplement. Cultures were routinely immunocytochemically stained with antibodies specific for neurons (β-tubulin III), astrocytes (glial fibrillary acidic protein), oligodendrocytes (myelin basic protein), and microglia (BS-lectin1); this protocol has routinely yielded cultures that are 90–95% neuronal. The neurons were maintained for 4–6 days before experimental manipulation. Before treatment with DETA-NO, the cultures were washed with PBS, exposed to drug diluted in Neurobasal A plus B27 for 3 h, rinsed with several volumes of PBS, followed by replacement with culture media, and viability was assessed after 16 h. Cortical neurons were treated with H_2O_2 in culture media, and viability was assessed 16 h later. Neuronal viability was assessed by using the Biotium assay kit for live/dead animal cells (Biotium, Hayward, CA).

Assessment of Mitochondrial Ca^{2+} Uptake. Mitochondria were prepared from WT and CyPD-KO brains following Ficoll gradient fractionation by using standard protocols (50). The Ca^{2+} retention capacity of mitochondria was assessed as outlined in ref. 30. In brief, experiments were started by the addition of 1 mg of mitochondrial protein to 2 ml of standard reaction buffer in the presence of the low-affinity Ca^{2+} indicator Calcium Green 5N. Fluorescence (extinction 506, emission 532) was followed as successive 2.5 μM pulses of Ca^{2+} were added at 1-min intervals.

We thank Jon Gross, Micha Rahder, and Katie Stern for excellent technical assistance. This work was supported by grants from the National Institutes of Health (M.F.), the Laura Fund for Innovation in Multiple Sclerosis Research (M.F.), the Department of Veterans Affairs (D.B.), and the Nancy Davis Center Without Walls (D.B.).

1. Frohman EM, Racke MK, Raine CS (2006) *N Engl J Med* 354:942–955.
2. Waxman SG (2002) *Arch Neurol (Chicago)* 59:1377–1380.
3. Waxman SG, Craner MJ, Black JA (2004) *Trends Pharmacol Sci* 25:584–591.
4. Bjartmar C, Trapp BD (2001) *Curr Opin Neurol* 14:271–278.
5. Trapp BD, Peterson J, Ransohoff RM, Rudick R, Mork S, Bo L (1998) *N Engl J Med* 338:278–285.
6. Silber E, Sharief MK (1999) *J Neurol Sci* 170:11–18.
7. Trapp B, Ransohoff R, Fisher E, Rudick R (1999) *Neuroscientist* 5:48–57.
8. De Stefano N, Matthews PM, Fu L, Narayanan S, Stanley J, Francis GS, Antel JP, Arnold DL (1998) *Brain* 121:1469–1477.
9. Stys PK (2005) *J Neurol Sci* 233:3–13.
10. Dutta R, McDonough J, Yin X, Peterson J, Chang A, Torres T, Gudz T, Macklin WB, Lewis DA, Fox RJ, *et al.* (2006) *Ann Neurol* 59:478–489.
11. Smith KJ, Lassmann H (2002) *Lancet Neurol* 1:232–241.
12. Gilgun-Sherki Y, Melamed E, Offen D (2004) *J Neurol* 251:261–268.
13. Stys PK, Waxman S (2005) in *Multiple Sclerosis As a Neuronal Disease*, ed Waxman S (Elsevier Academic, Amsterdam), pp 275–292.
14. Brookes PS, Yoon Y, Robotham JL, Anders MW, Sheu SS (2004) *Am J Physiol* 287:C817–C833.
15. Nicholls DG (2005) *Cell Calcium* 38:311–317.
16. Bernardi P (1999) *Physiol Rev* 79:1127–1155.
17. Bernardi P, Krauskopf A, Basso E, Petronilli V, Blachly-Dyson E, De Lisa F, Forte M (2006) *FEBS J* 273:2077–2099.
18. Huser J, Rechenmacher CE, Blatter LA (1998) *Biophys J* 74:2129–2137.
19. Petronilli V, Miotto G, Canton M, Brini M, Colonna R, Bernardi P, Di Lisa F (1999) *Biophys J* 76:725–734.
20. Petronilli V, Penzo D, Scorrano L, Bernardi P, Di Lisa F (2001) *J Biol Chem* 276:12030–12034.
21. Szabo I, Zoratti M (1991) *J Biol Chem* 266:3376–3379.
22. Di Lisa F, Bernardi P (1998) *Mol Cell Biochem* 184:379–391.
23. Friberg H, Wieloch T (2002) *Biochimie* 84:241–250.
24. Irwin WA, Bergamin N, Sabatelli P, Reggiani C, Megighian A, Merlini L, Braghetta P, Columbaro M, Volpin D, Bressan GM, *et al.* (2003) *Nat Genet* 35:367–371.
25. Nicolli A, Basso E, Petronilli V, Wenger RM, Bernardi P (1996) *J Biol Chem* 271:2185–2192.
26. Basso E, Fante L, Fowlkes J, Petronilli V, Forte MA, Bernardi P (2005) *J Biol Chem* 280:18558–18561.
27. Schinzel AC, Takeuchi O, Huang Z, Fisher JK, Zhou Z, Rubens J, Hetz C, Danial NN, Moskowitz MA, Korsmeyer SJ (2005) *Proc Natl Acad Sci USA* 102:12005–12010.
28. Baines CP, Kaiser RA, Purcell NH, Blair NS, Osinska H, Hambleton MA, Brunskill EW, Sayen MR, Gottlieb RA, Dorn GW, *et al.* (2005) *Nature* 434:658–662.
29. Nakagawa T, Shimizu S, Watanabe T, Yamaguchi O, Otsu K, Yamagata H, Inohara H, Kubo T, Tsujimoto Y (2005) *Nature* 434:652–658.
30. Kornek B, Storch MK, Weissert R, Wallstroem E, Stefferl A, Olsson T, Linington C, Schmidbauer M, Lassmann H (2000) *Am J Pathol* 157:267–276.
31. Gold R, Linington C, Lassmann H (2006) *Brain* 129:1953–1971.
32. Pitt D, Werner P, Raine CS (2000) *Nat Med* 6:67–70.
33. Charcot M (1868) *Histologie de la Sclerose en Plaques* (Gazette des hôpitaux, Paris) 141:554–555.
34. Steinman L (1999) *Neuron* 24:511–514.
35. Steinman L, Zamvil SS (2006) *Ann Neurol* 60:12–21.
36. Friese MA, Montalban X, Willcox N, Bell JI, Martin R, Fugger L (2006) *Brain* 129:1940–1952.
37. Chabas D, Baranzini SE, Mitchell D, Bernard CC, Rittling SR, Denhardt DT, Sobel RA, Lock C, Karpuj M, Pedotti R, *et al.* (2001) *Science* 294:1731–1735.
38. Jansson M, Panoutsakopoulou V, Baker J, Klein L, Cantor H (2002) *J Immunol* 168:2096–2099.
39. Komiyama Y, Nakae S, Matsuki T, Nambu A, Ishigame H, Kakuta S, Sudo K, Iwakura Y (2006) *J Immunol* 177:566–573.
40. Farrell R, Heaney D, Giovannoni G (2005) *Expert Opin Emerg Drugs* 10:797–816.
41. Kanwar JR (2005) *Curr Med Chem* 12:2947–2962.
42. Zhao GJ, Li DK, Wolinsky JS, Koopmans RA, Mietlowski W, Redekop WK, Riddehough A, Cover K, Paty DW (1997) *J Neuroimaging* 7:1–7.
43. Gold BG, Voda J, Yu X, McKeon G, Bourdette DN (2004) *J Neurosci Res* 77:367–377.
44. The Multiple Sclerosis Study Group (1990) *Ann Neurol* 27:591–605.
45. Hansson MJ, Mattiasson G, Mansson R, Karlsson J, Keep MF, Waldmeier P, Ruegg UT, Dumont JM, Besseghir K, Elmer E (2004) *J Bioenerg Biomembr* 36:407–413.
46. Waldmeier PC, Zimmermann K, Qian T, Tintelnot-Blomley M, Lemasters JJ (2003) *Curr Med Chem* 10:1485–1506.
47. Masliah E, Mallory M, Hansen L, Alford M, DeTeresa R, Terry R (1993) *Am J Pathol* 142:871–882.
48. Uo T, Kinoshita Y, Morrison RS (2005) *J Biol Chem* 280:9065–9073.
49. Xiang H, Hochman DW, Saya H, Fujiwara T, Schwartzkroin PA, Morrison RS (1996) *J Neurosci* 16:6753–6765.
50. Nicholls DG (1978) *Biochem J* 170:511–522.